Computational Materials Science 46 (2009) 600–602

Contents lists available at ScienceDirect

Computational Materials Science

journal homepage: www.elsevier.com/locate/commatsci

Modeling of micro-crack growth during thermal shock based on microstructural images of thermal barrier coatings

Shen Wei, Fan Qun-bo *, Wang Fu-chi, Ma Zhuang

School of Materials Science and Engineering, Beijing Institute of Technology, Beijing 100081, PR China

A R T I C L E   I N F O

Article history:
Received 11 November 2008
Received in revised form 23 February 2009
Accepted 31 March 2009
Available online 2 May 2009

PACS:
46.50.+a
47.11.Fg

Keywords:
Microstructural image of TBCs
Digital image processing
Finite element grid model
Micro-crack growth
Thermal shock

A B S T R A C T

Based on digital image processing theory and finite element mesh generation principle, a methodology is proposed to model the micro-crack growth of thermal barrier coatings (TBCs) during thermal shock with the aid of finite element program. Firstly, a microstructural image of plasma sprayed TBCs is transferred to digital image; secondly, a finite element grid model is generated by thresholding segmentation according to the actual microstructure; finally, based on the finite element grid model, the Tuler–Butcher failure criterion is employed to model the micro-crack growth of TBCs during thermal shock. The numerical simulation result agrees well with the experimental result, and the methodology presented in this paper is found to be effective to model the micro-crack growth.

1. Introduction

TBCs have been widely used as insulators for load-carrying hot components in industry. Due to the low thermal conductivity, ceramic, normally yttria stabilized zirconia (YSZ), is used as a top coat (TC) together with a metallic bond coat (BC). Here the TC acts as the thermal insulator while the BC provides adherence for the ceramic outer layer [1]. Since TBCs consist of a complex microstructure of particles with voids and micro-cracks in irregular [2], the properties of the coatings depend significantly on the heterogeneous morphology. Meanwhile, spontaneous microcracking during thermal shock has usually been observed, and such phenomenon can be attributed to misfit strains due to high temperature gradient, different coefficients of thermal expansion (CTE) and the existence of various defects.

The spontaneous micro-crack occurs due to thermal stresses, and it plays an important role in the failure of the whole coating. Recently, failures in TBCs have been extensively studied with finite element method (FEM). In Ref. [3], a bi-material structure containing an interfacial crack and subjected to a cooling shock, was investigated using the finite element method, based on a quasi-static uncoupled thermo-elasticity assumption. Gan and Ng [4] took use of indefective finite element models to simulate the stress development of TBCs during thermal shock cycling. Though, some achievements have been made by them, modeling based on the real microsturcture of TBCs has not been investigated. Digital image-based modeling has been applied to the heterogeneity analysis of TBCs. Recently, in Ref. [5], effects of pores and interfaces on effective properties of plasma sprayed zirconia coatings was studied based on a finite element model constructed with object oriented finite method (OOF) [6]. Michlik and Berndt [2] employed a new extended FEM program to predict the effective Young' modulus and assess the fracture behavior of the coating. However, up to the present time, modeling the micro-crack growth of TBCs by dynamic fracture criterion during thermal shock based on the true microstructure is not included in recent researches yet.

In this study, we present a methodology to generate a finite element grid model based on the true microstructure of TBCs. With the aid of finite element program, the proposed method is used to model the micro-crack growth of TBCs during thermal shock by the Tuler–Butcher criterion [7,8].

2. Digital image processing of TBCs microstructure

2.1. The digital image from microstructures of TBCs

A typical microstructure of plasma sprayed TBCs from the cross-section view by scanning electron microscopy (SEM) is shown in

* Corresponding author. Tel.: +86 10 68912712.
E-mail address: fanqunbo@bit.edu.cn (F. Qun-bo).

0927-0256/$ - see front matter © 2009 Elsevier B.V. All rights reserved.
doi:10.1016/j.commatsci.2009.03.039

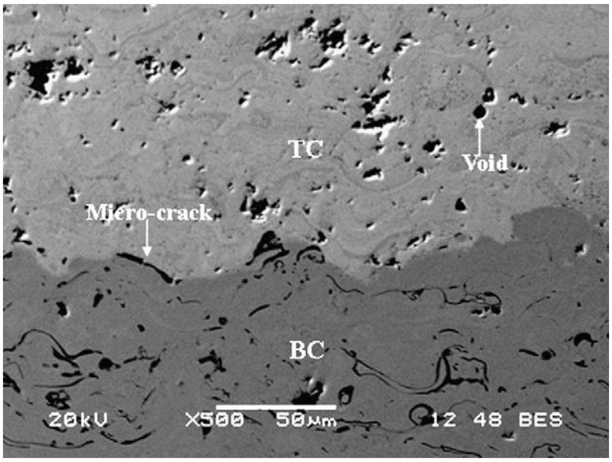

Fig. 1. The cross-section microstructure of TBCs.

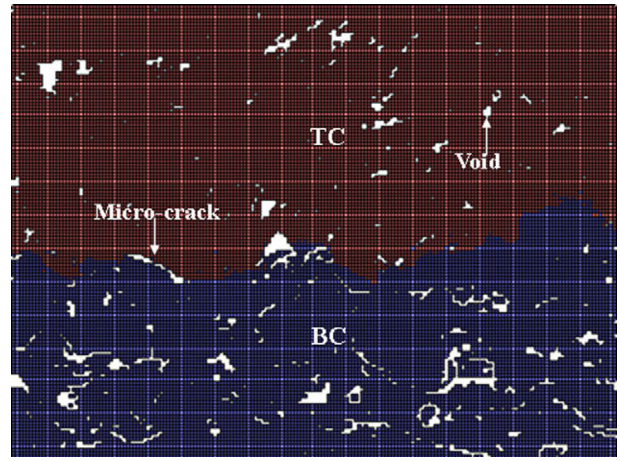

Fig. 2. The finite element grid model of TBCs (180×135).

Fig. 1. The model size is 240 μm × 180 μm. It includes YSZ TC and NiCoCrAlY BC with the dark color indicating defects of voids and micro-cracks. Such an image can be transferred to a digital image by digital image processing technology.

An image may be defined as a two-dimensional function *f*(*x*,*y*), where *x* and *y* are plane coordinates, and the amplitude of *f* at any pair of coordinates (*x*,*y*) is called the gray level of the image at that point. When *x*,*y* and the amplitude values *f* are all finite and discrete quantities, the image is a digital image. To create a digital image, the continuous sensed data should be converted into digital form. The digital image is compound of pixels, with one pixel corresponding to one gray level. Assume that an image *f*(*x*,*y*) is sampled so that the resulting digital image has *M* rows and *N* columns, the values of the coordinates (*x*,*y*) now become discrete quantities, integer values for these discrete coordinates, thus, the values of the coordinates at the origin are $(x,y) = (1,1)$. So the complete $M \times N$ digital image is written as the following compact matrix form [9]:

$$f(x,y) = \begin{bmatrix} f(1,1) & f(1,2) & \cdots & f(1,\mathrm{N}) \\ f(2,1) & f(2,2) & \cdots & f(2,\mathrm{N}) \\ \vdots & \vdots & \vdots & \vdots \\ f(\mathrm{M},1) & f(\mathrm{M},2) & \cdots & f(\mathrm{M},\mathrm{N}) \end{bmatrix} \tag{1}$$

The right side of this equation is by definition a digital image, each element of this matrix array is corresponding to a pixel, and every pixel holds only one gray level. Transferring the microstructural image of TBCs to digital image by digital image processing technology, and the digital image is the basis for thresholding segmentation.

2.2. Thresholding segmentation

Suppose Fig. 1 corresponds to an image *f*(*x*,*y*), composed of YSZ, NiCoCrAlY and defects, in such a way that these materials pixels have gray levels grouped into three modes. One obvious way to extract one from the others is to select thresholding *T* that separates these modes. Then any point (*x*,*y*) for which *f*(*x*,*y*) ε $[T_{n-1},T_n]$ is assigned to an appointed material label, where *n* is material number.

Thresholding may be viewed as an operation that involves tests against a function *T* of the form [9]:

$$T = T[(x,y), f(x,y), p(x,y)] \tag{2}$$

where *f* (*x*,*y*) is the gray level of point (*x*,*y*) and *p*(*x*,*y*) denotes some local property of this point.

Because there are three kinds of materials in Fig. 1, firstly, transferring the picture to a gray image, and then the image is identified as three parts by the gray levels with the following equation.

$$f(x,y) = \begin{cases} 1 & f(x,y) \in [0,T_1] \\ 2 & f(x,y) \in (T_1,T_2] \\ 3 & f(x,y) \in (T_2,255] \end{cases} \tag{3}$$

T reflects the thresholding of gray level, pixels labeled 1 represent defects; pixels labeled 2 are NiCoCrAlY; pixels labeled 3 are YSZ. In Eq. (3), T_1 is 30, and T_2 is 75.

2.3. Generation of a finite element grid model

Essentially, a digital image is collection of pixels, and a finite element model is collection of finite elements. With one pixel corresponding to one finite element, the collection of pixels can be changed to collection of finite elements. In addition, different gray levels reflect different materials. In this way, a finite element grid model in Fig. 2 based on the actual microstructure of TBCs is generated by thresholding segmentation and finite element mesh generation principle.

This finite element model is made up of 180×135 finite elements, and the dimensions are 240 μm × 180 μm.

3. Thermal shock and cracking of TBCs

Numerical simulation is performed with 2D model using LS-DYNA [10] to model micro-crack growth of the TBCs during thermal shock. A transient heat transfer analysis is carried out to account the thermal stresses. The top of the micrograph is heated alternately to 1000□ and followed by water-quenching to ambient temperature, so that a thermal gradient is built up in the direction of the expected heat flow. The other three sides of the model are kept adiabatic. In our simulation, the *MAT_ELASTIC_PLASTIC_THERMAL model is chosen to model the TC and BC materials. This material model allows for the definition of temperature dependent material coefficients in a thermo-elastic-plastic material. The YSZ material behavior is defined as linear elastic in Table 1 with a failure condition determined by the Tuler–Butcher failure criterion. It has been found that the dynamic mechanical resistance increase displays more importance for the brittle materials than the ductile materials [11]. To describe such behavior, Tuler and Butcher proposed a dynamic fracture criterion by the fracture time and maximum stress in materials [8]. According to them, the fracture phenomenon is

Table 1
Material properties of YSZ used in FEM model.

Density	Specific heat	Thermal conductivity	Thermal expansion	Young' modulus	Poisson's ratio
6300 kg/m^3	580 J/kg K	2.3 W/m K	11E-6(°C^{-1})	210 GPa	0.3

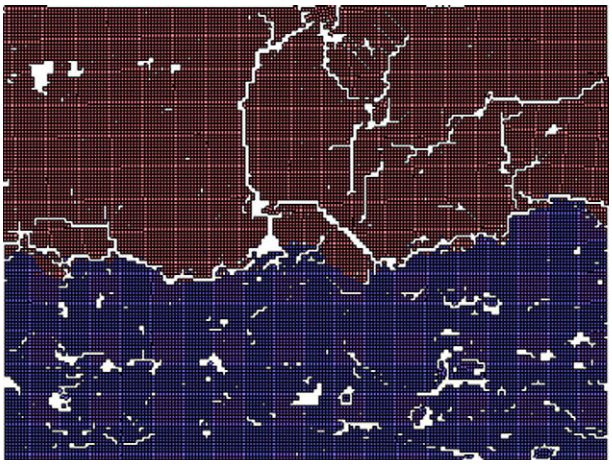

Fig. 3. Simulation result of micro-crack growth after 25 thermal shock cycles.

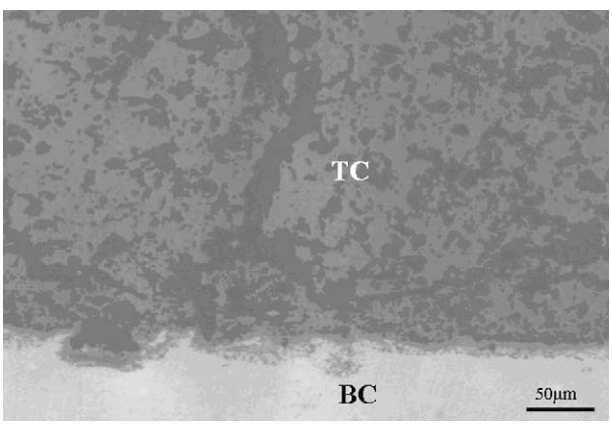

Fig. 4. Experimental result of crack growth after 25 thermal shock cycles.

not instantaneous but it requires necessary time duration to fracture. Hence, this cumulative damage concept can be described as

$$\int_0^t [\max(0, \sigma_1 - \sigma_0)]^2 dt \geqslant K_f \tag{4}$$

where σ_1 is the maximum principal stress, σ_0 is a specified threshold stress, $\sigma_1 \geqslant \sigma_0 \geqslant 0$, and$K_f$ is the stress impulse for failure. Stress values below the threshold value are too low to cause fracture even for very long duration loadings. In our simulation, σ_0 is 215 MPa, and K_f is 0.38 MPa^2 s.

During the simulation, the element satisfied with failure criterion is deleted from the model, so the micro-crack growth of TBCs during thermal shock is observable in the simulation.

4. Results and discussion

After 25 thermal shock cycles, the micro-crack growth caused by high temperature gradient and different CTE is shown in Fig. 3. Comparing with Fig. 2, damage evolution is obvious. Transverse cracks in the interface of TC and BC are generated mainly by different CTE between YSZ and NiCoCrAlY. Due to high temperature gradient and the existence of defects, the tensile stresses in the horizontal direction are induced during thermal shock, so vertical cracks initiated in the TC are developed, thus causing spallation of the TC finally. The presence of vertical cracks can relieve residual stress, thus enhance TBCs thermal shock resistance and prevent further delamination of TC. However, the large delamination crack in the TC makes it transparent to oxygen, and hence the thermally grown oxide (TGO) is easily formed at the interface of the TC and BC during high-temperature exposure. The TGO can also lead to the failure of the TBCs, such discussion is out of the scope of this paper.

Different from Fig. 1 which is used for computation and generated from the specimen before thermal shock loading, Fig. 4 shows the experimental result after thermal shock. However, they were taken from approximately the same position in the specimens and have undergone the same thermal shock condition. As shown in Figs. 3 and 4, a comparison between experimental results and numerical results shows that after 25 thermal shock cycles, the crack growth in simulation result agrees well with the corresponding experimental result. The methodology in our present work is effective to model the micro-crack growth.

5. Conclusions

In this paper, finite element mesh generation principle combined with digital image processing approach has been used to generate the finite element grid model based on the actual microstructural images of TBCs. With a failure condition determined by the Tuler–Butcher failure criterion, LS-DYNA code is employed to model micro-crack growth of the TBC during thermal shock. Numerical simulation results agree well with experimental results. Different from the traditional continuous indefective medium-based approach, the methodology presented in this paper is found to be more effective to model the micro-crack growth in TBCs, which is expected to be also available for predicting the life of the whole coatings in future study.

Acknowledgment

This paper is supported by NSFC (50801005).

References

[1] H. Brodin, M. Jinnestrand, S. Johansson, S. Sjöström, Thermal barrier coating fatigue life assessment, Siemens AG, 2006.
[2] P. Michlik, C. Berndt, Surface and Technology 201 (2006) 2369–2380.
[3] D.E. Katsareas, G.I. Giannopoulos, N.K. Anifantis, Computers and Structures 84 (2006) 1958–1964.
[4] Z. Gan, H.W. Ng, Materials Science and Engineering A 385 (2004) 314–324.
[5] Z. Wang, A. Kulkarni, S. Deshpande, T. Nakamura, H. Herman, Acta Materialia 51 (2003) 5319–5334.
[6] S.A. Langer, W.C. Carter, E.R. Fuller, National Institute of Standards and Technology (1998) 2–8.
[7] B.M. Butcher, L.M. Barker, D.E. Munson, C.D. Lundergan, AIAA (1964).
[8] Floyd R. Tuler, Barry M. Butcher, The International Journal of Fracture Mechanics 4 (1968) 431–437.
[9] Rafael C. Gonzalez, Richard E. Woods, Digital Image Processing, Pearson/ Prentice Hall Press, Upper Saddle River, 2007.
[10] LS-DYNA Key word user's manual. Livermore Software Technology Corporation, <http://www.lstc.com>.
[11] J. Jeong, H. Adib, G. Pluvinage, Journal of Non-Crystalline Solids 351 (2005) 2065–2075.